In Situ Study of the Growth Kinetics of Individual Island Electrodeposition of Copper

A. Radisic,[†] F. M. Ross,*[,‡] and P. C. Searson*[,†]

Department of Materials Science and Engineering, Johns Hopkins University, Baltimore, Maryland 21218, and T. J. Watson Research Center, IBM, Yorktown Heights, New York 10598

Received: December 28, 2005; In Final Form: February 17, 2006

The growth kinetics for individual islands during electrodeposition of copper have been studied using in situ transmission electron microscopy. We show that for sufficiently large overpotentials, the growth kinetics approach the rate laws expected for diffusion-limited growth of hemispherical islands, characterized by two distinct regimes. At short times, the island growth exponent is 0.5 as expected for diffusion-limited growth of uncoupled hemispherical islands, while at longer times, the growth exponent approaches $^1/_6$ as expected for planar diffusion to the growing islands. These results provide the first direct measurements of the growth of individual islands during electrochemical deposition. However, quantitative comparison with rate laws shows that the island radii are smaller than predicted and the island densities are much larger than predicted, and we suggest that this is related to adatom formation and surface diffusion, processes which are not included in conventional growth models.

Introduction

In electrochemical deposition, film growth at potentials positive to the equilibrium potential (underpotential deposition) occurs through formation of two-dimensional (2D) islands and can be imaged by scanning probe microscopy.[1,2] However, three-dimensional (3D) island growth at potentials negative to the equilibrium potential (overpotential or bulk deposition) cannot be examined using these techniques due to the limited dynamic range, tip−surface interactions, and limitations in imaging surfaces with large height variations. As a result, there have been very few studies of island growth during overpotential deposition. Instead, studies of island growth have been limited to analysis of deposition current transients recorded during growth at constant potential. Since the current is proportional to the flux of atoms at the surface, the island growth rate averaged over all islands at the surface can be inferred from the current transients.[3−6] While this approach can be useful in determining the mechanism of growth in certain limiting cases,[7] for a detailed analysis of growth mechanisms it is essential to image the growth of individual islands. Ex situ imaging can be used to study the island growth kinetics[8,9] but cannot be used to track the growth of an individual island. Furthermore, this approach is exceedingly time-consuming, requiring a separate sample for each data point.

Here we report on the growth of individual islands during bulk electrodeposition of copper as a function of potential using in situ transmission electron microscopy (TEM). By carrying out deposition in a small electrochemical cell within the microscope, we obtain a continuous series of images of the same area of the electrode. This allows us to follow the progress of individual islands up to coalescence. In previous work,[10] we have examined the nucleation process, showing that the kinetics are first-order although they cannot be approximated to the limiting cases of progressive or instantaneous nucleation which are often assumed. In this paper, we present the growth kinetics of individual islands. We show the dependence of island radii on time both at large overpotentials, where the growth is limited by diffusion, and at small overpotentials, where the growth is limited either by the surface reaction (kinetically limited) or by both processes (mixed control). We show that at large overpotentials the overall form of the growth kinetics does indeed follow the predictions expected for a diffusion-limited process, while the kinetics deviate from these predictions at small overpotentials. These results provide the first direct verification of diffusion control for individual islands during overpotential deposition. However, a more detailed and quantitative comparison of the island growth rates with the diffusion-limited predictions highlights a surprising discrepancy in the magnitude of the growth rates: islands grow far more slowly than expected. Similarly, the density of islands is very different from the predictions of growth models, being much higher. We show that conventional electrochemical growth models, in which islands grow by the diffusion of ions through the solution, must be modified to agree with the data, and we suggest that the direct attachment of ions to the electrode followed by surface diffusion to the islands dominates at early times.

Experimental Section

In Situ Microscopy and Image Analysis. All experiments were performed in a sealed, thin layer electrochemical cell in which a layer of liquid was enclosed between two thin Si_3N_4 windows 1−2 μm apart, one of which was patterned with the working electrode. The solution, electrode, and windows were thin enough to be transparent to the 300 kV electrons used for imaging in the TEM. The working electrode was polycrystalline Au with a total area of 2×10^{-5} cm^2, while the reference electrode (a copper wire) and the counter electrode (a gold wire) were located in two solution reservoirs on each side of the electron transparent area. All potentials are reported with respect to the Cu wire reference electrode. Further details of the cell fabrication can be found elsewhere.[11,12] The experiments were

* To whom correspondence should be addressed. E-mail: fmross@us.ibm.com and searson@jhu.edu.
[†] Johns Hopkins University.
[‡] IBM.

10.1021/jp057549a CCC: $30.25
Published on Web 03/25/2006

performed in a solution containing 0.1 M $CuSO_4 \cdot 5H_2O$ (J. T. Baker) and 1 vol % H_2SO_4 (J. T. Baker).

During operation of this cell within the electron microscope (a Hitachi H-9000 operating at 300 kV), images of a small area of the electrode ($\sim 1\ \mu m \times 2\ \mu m$) were recorded at a video rate (30 frames per second). Images were acquired in bright field conditions so that the Cu islands appeared as dark areas on a uniform background; individual grains of the gold electrode were not visible. These imaging conditions provided excellent contrast, even though multiple scattering of electrons by the electrolyte and windows provided a large background in the images. For analysis of the growth rates of individual islands, separate frames were extracted from the videos and each frame was thresholded and segmented to identify the location and size of each island present. Software that allowed individual islands to be tracked automatically from one frame to the next was used. The growth rate of individual islands was determined from the time evolution of the effective island radius, defined as the radius of a circle having the same area as the projected island area. In calculations and modeling, the islands were assumed to be hemispherical, an assumption that was supported by postgrowth AFM imaging.

Results and Discussion

Identification of the Diffusion-Limited and Mixed Regimes. The operation of the electrochemical cell was initially verified by performing cyclic voltammetry.[10] Figure 1 shows a typical voltammogram recorded in the TEM column illustrating a characteristic nucleation and diffusion-limited growth peak at −0.095 V, and a stripping peak at 0.11 V on the reverse scan. The distortion of the voltammogram around 0 V is associated with the relatively high contact resistance to the working electrode in the cell and is not related to electrochemical processes. Subsequent scans (not shown) revealed excellent reproducibility, and the peak positions were in good agreement with voltammograms recorded at large area electrodes. These results indicate that growth is under kinetic or mixed control in the potential range from −0.05 to ca. −0.07 V and is diffusion-limited at potentials negative to ca. −0.07 V.

The growth of islands was examined at constant potential, with values ranging from −0.05 to −0.1 V, as indicated in the voltammogram. In Figure 1, we show a representative series of TEM images and the corresponding current−time response recorded at −0.09 V, close to the diffusion-limited deposition peak in the current−voltage curve. In the current transient, we see that the deposition current initially increases to -5.6×10^{-7} A after 0.4 s and subsequently decreases at longer times. These features are characteristic of nucleation and diffusion-limited growth: at short times, the increasing current is associated with the growth of noninteracting 3D islands, while at longer times, the diffusion fields of individual islands overlap resulting in a transition to planar diffusion of copper ions to the growing islands and a decrease in the current.

At long times, for the case of one-dimensional (1D) diffusion-limited growth from a planar diffusion field, the deposition current is given by the Cottrell equation

$$i(t) = \frac{zFD^{1/2}c_b}{\pi^{1/2}t^{1/2}} \quad (1)$$

where z is the charge on the ion, F is Faraday's constant, c_b is the bulk ion concentration, and D is the diffusion coefficient for ions in bulk solution. Figure 2 shows a plot of I^{-2} versus t for the current−time transient at −0.09 V shown in Figure 1.

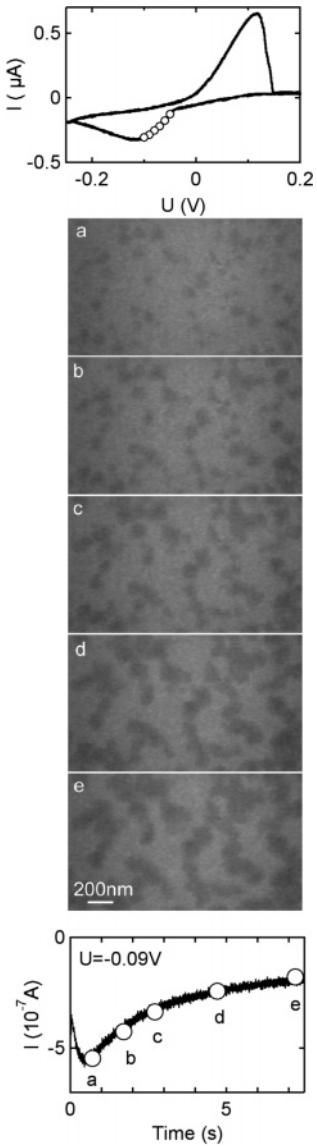

Figure 1. (Top) Current−voltage curve for copper deposition and stripping on gold in 0.1 M $CuSO_4 \cdot 5H_2O$ and 1 vol % H_2SO_4. The data were recorded in a sealed cell in the TEM column at a scan rate of 25 mV/s. (Center) Bright field images of part of the electrode are shown after (a) 0.7, (b) 1.7, (c) 2.7, (d) 4.7, and (e) 7.2 s at −0.09 V. The field of view for each image is $1.85\ \mu m \times 1.42\ \mu m$. (Bottom) Current−time plot for deposition at a constant potential of −0.09 V.

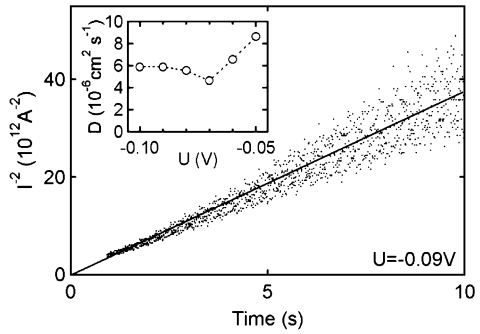

Figure 2. (a) Deposition current transient at −0.09 V shown in Figure 1 replotted as I^{-2} vs t. The inset shows the diffusion coefficient obtained from the slopes of I^{-2} vs t plots at deposition potentials from −0.05 to −0.1 V.

The diffusion coefficient obtained from the slope is 6×10^{-6} $cm^2\ s^{-1}$, in excellent agreement with the value reported in the

literature.[13] The inset shows that the diffusion coefficients obtained by performing a similar analysis on data recorded at potentials from −0.07 to −0.1 V are also very close to the literature value. At more positive potentials, the apparent diffusion coefficients obtained from the slopes are somewhat higher, characteristic of mixed control. These results provide further confirmation that the growth kinetics are diffusion-limited at potentials negative to −0.07 V, while under mixed kinetic/diffusion control at more positive potentials.

In the analysis of nucleation and growth, we must consider the geometry of the cell imposed by the requirement for an electron transparent window. In the early stages of nucleation and growth, up to the current maximum in the deposition transients, the hemispherical diffusion zones around each island are noninteracting. The maximum radius of the isolated hemispherical diffusion zones is approximately $N^{-1/2}/2$, where N is the island density. In our experiments, the maximum radius ranges from 360 nm at −0.6 V to 80 nm at −1.0 V, smaller than the thickness of the cell in the electron transparent window. The rate of build up of the diffusion field once the individual diffusion zones begin to interact is dependent on the island density (or nucleation rate). At long times and large overpotentials (high island density), we would expect ion depletion to extend to the silicon nitride window above the working electrode and then laterally to the solution reservoirs on either side. The transition from vertical to lateral transport is difficult to predict since it is dependent on the island density (or nucleation rate). Consequently, analysis of the deposition transients at long times must be performed with caution. However, in previous work,[10] we have demonstrated that the islands in the images ($A = 2.64 \times 10^{-8}$ cm^{-2}) are representative of the electrode area ($A = 2 \times 10^{-5}$ cm^{-2}) over the time scales of our experiments, indicating that there are no significant spatial differences in nucleation and growth across the surface. These results show that the geometry of the cell does not influence nucleation and growth, at least up to the time corresponding to the current peak in the transients.

Determination of the Growth Exponents for Individual Islands. From the sequence of images recorded during deposition, we can determine the growth rates for individual islands. Analysis was carried out in the following way. First, the island boundaries were determined by thresholding the images. The area of each island was then used to determine the effective radius R, corresponding to the radius of the circle with the same area. Plots of $R(t)$ versus time were then generated by tracking individual islands over a series of images. Note that islands smaller than 20−30 nm in diameter do not produce sufficient contrast in the images to be analyzed.

Before showing the growth rates for individual islands, we consider two limiting cases. At short times, we would expect island growth to follow diffusion-limited growth of an isolated hemispherical island, as long as the diffusion fields for individual islands do not interact. At longer times, when the islands compete for ions, we would expect island growth to follow 1D diffusion-limited growth from a planar diffusion field.

Assuming that direct attachment of ions to the growing island is the only process occurring at the surface, the growth of an isolated hemispherical island under diffusion control is given by[14]

$$R(t) = (2Dc_bV_mt)^{1/2} \tag{2}$$

where V_m is the molar volume (7.1 cm^3 mol^{-1}). As long as $c_bV_m \ll 1$, then radial convection can be neglected[14] and hence $R(t) \propto t^{1/2}$.

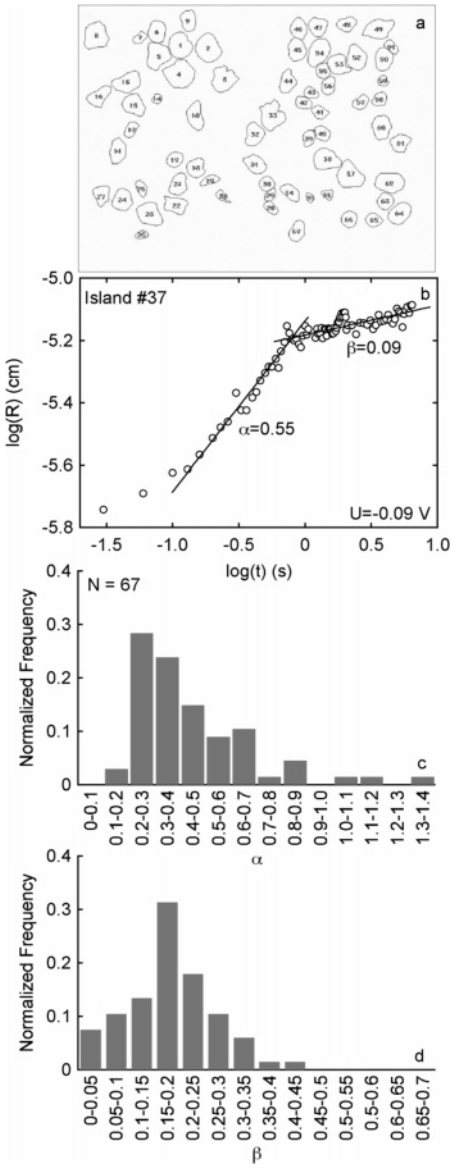

Figure 3. (a) Contour plot of copper islands after deposition for 1 s at −0.09 V (the image is 1.85 μm × 1.42 μm), (b) log(R) vs log(t) curve for growth of island 37, (c) distribution of growth exponent α, and (d) distribution of growth exponent β.

At long times, when the diffusion fields from neighboring islands have overlapped significantly, we obtain the case of 1D diffusion-limited growth from a planar diffusion field. In this situation, the charge q deposited after time t is given by

$$q = \int_0^t i\,dt = \int_0^t \frac{zFDc_b}{\pi^{1/2}t^{1/2}}\,dt = K_1t^{1/2} \tag{3}$$

where K_1 is a constant. From Faraday's law, the charge associated with a hemispherical island of volume $2\pi R^3/3$ is

$$q = \frac{2zF\pi}{3AV_m}R^3 = K_2R^3 \tag{4}$$

where A is the electrode area and K_2 is a constant. By comparing eqs 3 and 4, we see that that at long times, the time dependence of the radius of a hemispherical island for 1D diffusion-limited growth is expected to be $R(t) = (K_1/K_2)^{1/3}t^{1/6}$ or $R(t) \propto t^{1/6}$.

Figure 3a shows a contour plot of copper islands after 1 s deposition at −0.09 V. In the log(R)−log(t) plot (Figure 3b),

two growth regimes can indeed be identified. The growth exponent at short times $\alpha = 0.55$, and at longer times, the growth exponent $\beta = 0.09$. Note that the expected values are 0.5 and 0.167, respectively, so this island does appear to follow the diffusion-limited predictions reasonably well. Panels c and d of Figure 3 show the results of measuring the two growth exponents for all 67 islands in the image, and a distribution of values is apparent.

Various factors are expected to lead to a distribution of exponents. Two factors may influence the growth exponent at short times. One factor arises from the assumption that all islands are hemispherical. AFM imaging of the surface after deposition shows that this is approximately correct, although a small fraction of islands are spherical segments with a height shorter than the base radius. Islands whose center lies beneath the plane of the surface would be expected to have growth exponents slightly larger than that for a hemispherical island. A second factor is the interaction of the diffusion fields between islands that are very close. As demonstrated in Brownian dynamics simulations of island growth,[15] this effect is expected to give growth exponents of <0.5. At long times, other factors can influence the growth exponent. For example, the diffusion layer expands more slowly as the nucleation rate decreases, resulting in deviation from the Cottrell equation.[16] Thus, the distribution of near-neighbor distances and the time at which islands are born are expected to give rise to local differences in the diffusion fields and hence a distribution of growth exponents.

The same analysis can be carried out for sequences of images obtained at different potentials. Figure 4a shows a contour plot extracted from one frame of a movie after deposition at -0.08 V for 4.8 s. There are 30 islands in the field of view, illustrating the decrease in island density seen at more positive potentials. The $\log(R)-\log(t)$ plot in Figure 4b shows two growth regimes with exponents similar to those shown for deposition at -0.09 V. Panels c and d of Figure 4 show the corresponding distributions for the growth exponents. Similarly, Figure 5a shows the contour plot for deposition at -0.07 V after 2.2 s. The island density again decreases, with 16 islands in the field of view. Figure 5b shows a typical growth curve, and panels c and d of Figure 5 show the distributions of the growth exponents. Finally, at -0.06 V, the island density is very low and only two islands are seen in the image. Figure 6 shows a contour plot for deposition at -0.06 V after 9.5 s along with a radius versus time plot for the island in the center of the image. The island on the left coalesces with an island on the perimeter, and hence, analysis is not possible. The growth exponents for the central island are $\alpha = 0.65$ and $\beta = 0.33$.

In Figure 7, we collect the average growth exponents and plot them versus the deposition potential. From this, we see that α decreases from 0.65 at -0.06 V to 0.45 at -0.09 V. As described above, at -0.05 V the deposition process is under mixed kinetic/diffusion control whereas at more negative potentials deposition becomes diffusion-limited, and Figure 7 shows that α indeed approaches the diffusion-limited value of 0.5 at more negative potentials.

As described above, a growth exponent $\alpha = 0.50$ is expected only when the island density is sufficiently low that the diffusion fields of the individual islands do not interact at short times. If the island density is large, then there will be some competition for ions, even during the early stages of growth, and the growth exponent will decrease. In our experiments, the saturation island density N_0 increases from 1.9×10^8 cm^{-2} at -0.06 V to 4.3×10^9 cm^{-2} at -0.10 V, and hence, at some time the growth

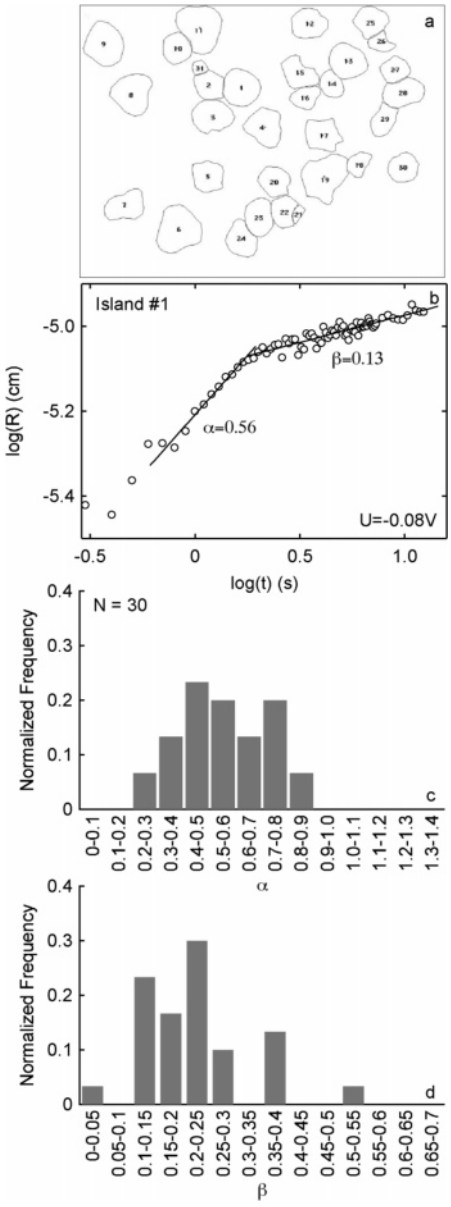

Figure 4. (a) Contour plot of copper islands after deposition for 4.8 s at -0.08 V (the image is 1.85 μm $\times$ 1.42 μm), **(**b**)** $\log(R)$ vs $\log(t)$ curve for growth of island 1, (c) distribution of growth exponent α, and (d) distribution of growth exponent β.

exponent is expected to decrease below 0.50. This effect may contribute to the average growth exponent of 0.45 at -0.09 V.

The growth exponent β decreases from 0.33 at -0.06 V to 0.18 at -0.09 V, very close to the value of $^1/_6$ (0.17) for diffusion-limited growth from a planar diffusion field. As described above, this is consistent with the growth mechanism expected at long times.

We therefore conclude that for potentials close to the diffusion-limited deposition peak in the current$-$voltage curve, the island growth exponents follow the rate laws $\alpha = 0.5$ and $\beta = 0.17$ expected for diffusion-limited growth. For small overpotentials, where both the voltammograms and the bulk diffusion coefficients obtained from the slopes of the $I^{-2}-t$ plots suggest that growth is in the mixed regime, we do indeed find that the growth exponents deviate from the diffusion-limited values. These exponents are expected to contain information about the precise physical processes that control growth at these potentials.

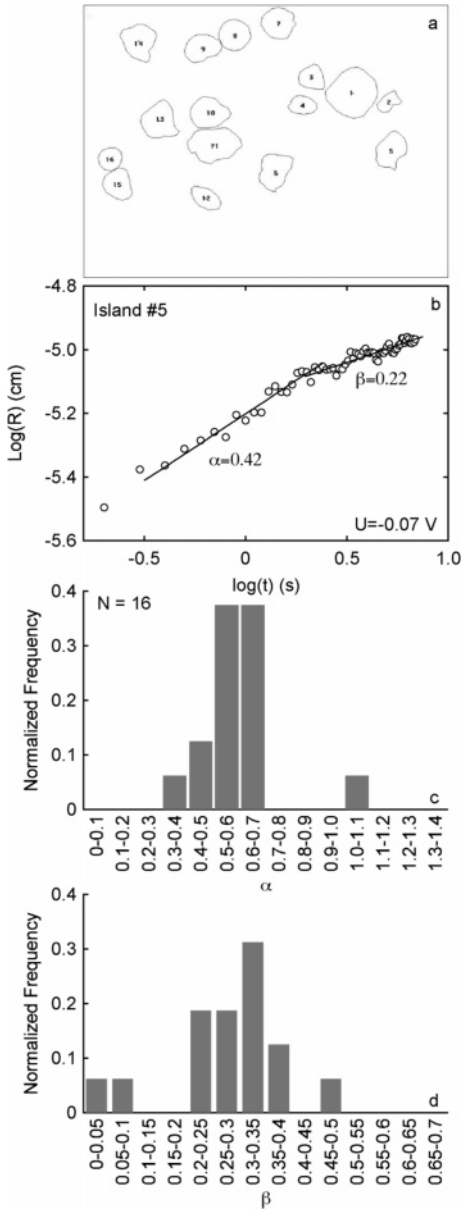

Figure 5. (a) Contour plot of copper islands after deposition for 2.2 s at −0.07 V (the image is 1.85 μm × 1.42 μm), **(**b**)** log(R) vs log(t) curve for growth of island 5, (c) distribution of growth exponent α, and (d) distribution of growth exponent β.

Determination of the Growth Prefactor. We now consider another aspect of the growth laws for individual islands, the prefactor. The following analysis is based on the fact that in eq 2 the island growth law at short times is determined exactly, provided the values of D and c_b are known. Thus, it is possible to compare the island growth rate quantitatively with the simple diffusion-limited growth model. Figure 8 shows a log(R)−log(t) plot for an island at −0.08 V along with the growth law according to eq 2. As described above, the slope during the early stages of deposition, up to t_{max}, is close to the value of 0.5 expected for the growth of an isolated island. However, comparison of the absolute values for the two curves shows that the island radius is ∼15 times smaller than that predicted from eq 2. In fact at every potential, we find that the island radii obtained from analysis of the images are 15−20 times smaller than that given by eq 2.

We first note that this surprising difference cannot be explained by assuming that the deposition reaction is under mixed kinetic/diffusion control. By definition, mixed control is

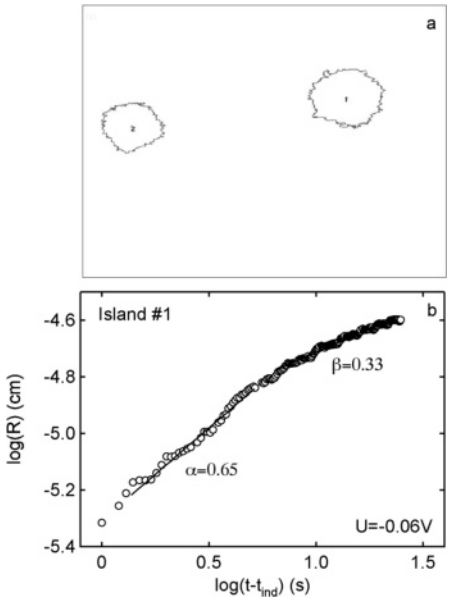

Figure 6. (a) Contour plot of copper islands after deposition for 9.5 s at −0.06 V (the image is 1.85 μm × 1.42 μm) and **(**b**)** log(R) vs log(t) curve for growth of island 1.

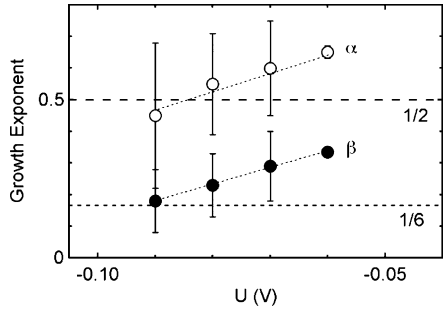

Figure 7. Average growth exponents vs the deposition potential. The error bars are calculated from the distributions of exponents given in Figures 3−5. Also indicated in the figure are the growth exponents for diffusion-limited growth of an isolated hemispherical island (exponent of $^1/_2$) and planar diffusion-limited growth (exponent of $^1/_6$).

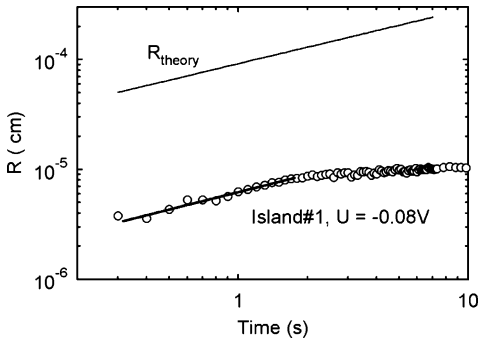

Figure 8. Comparison of a log(R) vs log(t) plot for growth of an island at −0.08 V along with the growth law according to eq 2. The straight line fit through the data at early times is the α = 0.5 growth law.

growth under conditions where the surface concentration of ions, c_s, is not zero (while for diffusion-limited growth, $c_s = 0$). For example, if the surface concentration of ions were $0.5c_b$, then the radii would be expected to be just 30% smaller, much less than the factor of 15−20 seen experimentally.

Furthermore, since the growth exponents for the noninteracting islands are consistent with diffusion-limited growth, the fact that the island radii are approximately 1 order of magnitude lower than predicted cannot be explained by an offset or

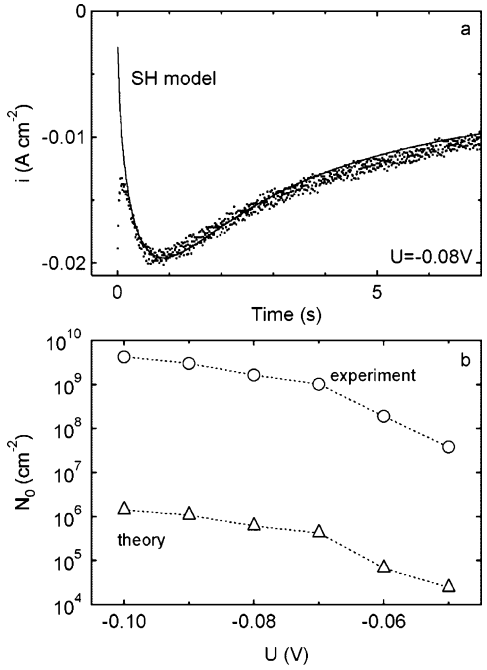

Figure 9. (a) Deposition current transient at −0.08 V and (—) fit to the Scharifker−Hills model using eq 5. (b) Island density obtained from (○) analysis of TEM images and (△) calculation from experimentally determined values of i_{max} and t_{max} using eq 6 with the following: $D = 6 \times 10^{-6}$ cm^2 s^{-1}, $V_m = 7.1$ cm^3 mol^{-1}, and $c_b = 0.1$ M.

incubation time in eq 2. Instead, one of the assumptions made in deriving eq 2 must be incorrect. Equation 2 implicitly assumes that island growth is limited by three-dimensional diffusion of ions to the islands from time zero and that the only electrochemical process is the direct attachment of ions to growing islands. However, at short times, other processes such as double-layer charging, adion or adatom formation, and surface diffusion may occur in parallel. We will discuss these processes in more detail below.

Comparison of Island Growth Laws to Current−Time Transients. So far, we have measured the growth of individual islands directly using information obtained from the TEM images. However, for each video sequence, the corresponding current transient provides a source of complementary information. We will now show that a comparison of the images and current transients leads to a second surprising discrepancy between diffusion-limited growth models and experimental data. Figure 9a shows the deposition transient at −0.08 V, along with a fit to the Scharifker−Hills (SH) model for instantaneous nucleation and diffusion-limited growth. According to the SH model, the deposition current density (normalized to the geometric surface area) is given by

$$i(t) = \frac{zFD^{1/2}c_b}{\pi^{1/2}t^{1/2}}\{1 - \exp[-N_0 D(8\pi^3 c_b V_m)^{1/2}t]\} \qquad (5)$$

where z is the valence of the metal ion, F is Faraday's constant, and N_0 is the island density. After the initial current decay at short times, we see that the SH model provides a good fit to the experiment.

From the SH model, the island density can be obtained from

$$N_0 = 0.065(8c_b V_m D)^{-1/2}\left(\frac{zFc_b}{i_{max}t_{max}}\right)^2 \qquad (6)$$

where t_{max} is the time corresponding to the current maximum i_{max} and in the transient. Figure 9b shows a comparison of the final island density obtained from analysis of the TEM images and the island density obtained from eq 6 using the values of i_{max} and t_{max} obtained from the deposition transients. The island density obtained from the TEM images increases from 4×10^7 to 4×10^9 cm^{-2} as the deposition potential is shifted from −0.05 to −0.1 V. The island density obtained from eq 6 exhibits the same dependence on potential, but the island densities are just more than 3 orders of magnitude lower, increasing from 2×10^4 to 1×10^6 cm^{-2} over the same potential range.

Thus, we find that the island density is 3 orders of magnitude larger than that predicted by the SH diffusion-limited growth model, and each island is approximately 1 order of magnitude smaller than predicted by the rate law for diffusion-limited growth of a single island. Conservation of mass requires that a 3 order of magnitude increase in the island density result in island radii that are 1 order of magnitude smaller than those predicted by eq 2. The island densities are from 2000 to 4000 times larger than those predicted by the SH model (Figure 9b), and hence, we expect that the island radii would be between 13 and 16 times smaller. As described above, the radii of the islands determined from the images at all potentials are 15−20 times smaller that those predicted by eq 2 (see Figure 8).

As noted above, the SH model assumes that metal ion reduction occurs only at the islands; i.e., growth occurs by the direct attachment of ions to the growing islands. The discrepancy between the island density and island radii indicates that this condition is not satisfied. Below, we discuss a parallel process for attachment to islands.

An Explanation Based on Adatom Adsorption. In many cases, deposition transients exhibit an initial current decay prior to the onset of the rising part of the nucleation and growth curve. The time constant of this initial decay is often greater than 1 ms and hence cannot be due to double-layer charging.[17,18] In our experiments, the deposition transients exhibit an initial exponential decay with a time constant in the range of 0.05−2 s. The exponential decay and relatively long time constant imply that a surface process such as the formation of adions or adatoms may be occurring in parallel with island growth by direct attachment. As islands nucleate and grow, the area available for adatom formation on the substrate by metal ion reduction decreases so that the contribution from this parallel current decreases. Simulations are required to model the contribution from parallel processes accurately. However, a very simple simulation which includes some aspects of this parallel process does indeed show island growth with the expected exponent of 0.5 but a lower prefactor.[19]

In Figure 10a, we show the deposition transient at −0.08 V, with its initial current decay. This initial decay has been fit to an adsorption equation of the form[20]

$$i(t) = C\exp(-k_{ads}t) \qquad (7)$$

where C is a constant and k_{ads} is the rate constant for adsorption. A background current of 3 mA cm^{-2}, determined from the transient at −0.05 V, was subtracted from the transient before fitting. As for any activated interfacial process, k_{ads} is expected to be potential-dependent. Figure 10b shows the values of the rate constant k_{ads} and the total charge associated with the initial decay part of the deposition transient versus the deposition potential. From this, it is seen that k_{ads} exhibits an exponential dependence on potential in the range from −0.07 to −0.1 V, as expected for an adsorption process.

This adsorption process can explain the differences in island density and growth rates obtained from TEM images and from

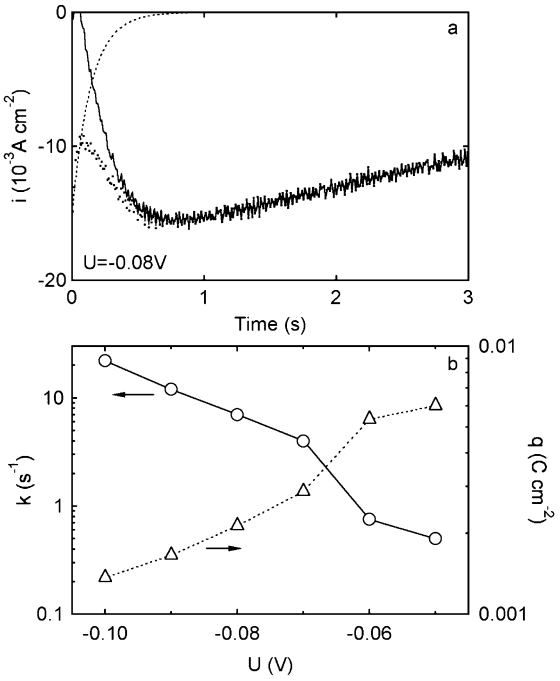

Figure 10. (a) Deposition current transient at −0.08 V with an exponential fit (···) to the initial decay part of the transient according to eq 7. The solid line shows the deposition current transient after subtraction of this initial exponential decay. (b) Adsorption rate constant k and adsorption charge q plotted vs deposition potential.

the diffusion-limited growth model. Adatoms generated by adsorption will result in the formation of additional islands, increasing the island density above the expected value, and the parallel adatom formation process would be expected to decrease the concentration of ions near the electrode and hence reduce the prefactor for individual island growth. Further detailed modeling is required to quantify the effects of a parallel adsorption process on the island nucleation density and growth rates.

Summary

We have examined the growth laws of individual copper islands on gold by direct observation during electrodeposition. The growth of individual islands is characterized by two growth exponents α and β. At short times, the diffusion fields associated with ion transport from the bulk solution to the growing island are noninteracting and the growth exponent $\alpha \rightarrow 0.5$, characteristic of 3D diffusion-limited growth of noninteracting hemispherical islands. At longer times, the diffusion fields interact and there is a transition to a growth exponent $\beta \rightarrow {}^{1}/_{6}$, corresponding to planar diffusion to the growing islands. These results provide the first direct measurements of growth exponents for individual islands during electrodeposition. The growth exponents are dependent on potential and asymptotically approach the expected limits with increasing overpotential, corresponding to the transition from mixed kinetic/diffusion control to pure diffusion control. Although the island growth rate laws can therefore be understood by conventional diffusion-limited growth models, the island radii are smaller than predicted and the island densities are much larger than predicted from models that assume only direct attachment of ions to the growing islands. We show that this is consistent with a parallel process of adatom formation and surface diffusion occurring at short times.

These results highlight the importance of direct observation for the characterization of nucleation and growth in electrodeposition. Analytical models, such as the SH model, are widely used to extract nucleation and growth parameters from macroscopic electrochemical measurements. However, the implicit assumptions made in these models are often difficult to verify. Our results show that the models do allow us to understand important features of nucleation and growth, such as the growth exponents, but we also show that key assumptions may not always be valid and, without additional development, the models cannot always provide reliable quantitative predictions for nucleation and growth kinetics, which are essential for understanding the microstructure of electrochemically deposited materials.

Acknowledgment. We acknowledge financial support from IBM through an IBM Faculty Award and an IBM Graduate Student Summer Internship and the Johns Hopkins University MRSEC (NSF Grant DMR05-20491). We also acknowledge M. C. Reuter, A. Ellis, and S. J. Chey for assistance with experimental aspects of this work and J. B. Hannon for stimulating discussions and for assistance with image analysis.

References and Notes

(1) Dietterle, M.; Will, T.; Kolb, D. M. *Surf. Sci.* **1995**, *342*, 29−37.
(2) Xia, X. H.; Nagle, L.; Schuster, R.; Magnussen, O. M.; Behm, R. J. *Phys. Chem. Chem. Phys.* **2000**, *2*, 4387−4392.
(3) Budevski, E.; Staikov, G.; Lorenz, W. J. *Electrochemical phase formation and growth*; VCH: New York, 1996.
(4) Gunawardena, G.; Hills, G.; Montenegro, I.; Scharifker, B. *J. Electroanal. Chem.* **1982**, *138*, 225−239.
(5) Scharifker, B.; Hills, G. *Electrochim. Acta* **1983**, *28*, 879−889.
(6) Hyde, M. E.; Compton, R. G. *J. Electroanal. Chem.* **2003**, *549*, 1−12.
(7) Oskam, G.; Vereecken, P. M.; Searson, P. C. *J. Electrochem. Soc.* **1999**, *146*, 1436−1441.
(8) Ji, C. X.; Oskam, G.; Searson, P. C. *Surf. Sci.* **2001**, *492*, 115−124.
(9) Oskam, G.; Searson, P. C. *Surf. Sci.* **2000**, *446*, 103−111.
(10) Radisic, A.; Searson, P. C.; Ross, F. M. *Surf. Sci.*, **2006**, in press.
(11) Ross, F. M.; Radisic, A.; Williamson, M. J.; Chey, S. J.; Tromp, R. M.; Reuter, M. C.; Ellis, A.; Hull, R.; Searson, P. C. **2005**, manuscript in preparation.
(12) Williamson, M. J.; Tromp, R. M.; Vereecken, P. M.; Hull, R.; Ross, F. M. *Nat. Mater.* **2003**, *2*, 532−536.
(13) Quickenden, T. I.; Xu, Q. Z. *J. Electrochem. Soc.* **1996**, *143*, 1248−1253.
(14) Fletcher, S. *J. Chem. Soc., Faraday Trans. I* **1983**, *79*, 467−479.
(15) Fransaer, J. L.; Penner, R. M. *J. Phys. Chem. B* **1999**, *103*, 7643−7653.
(16) Heerman, L.; Tarallo, A. *Electrochem. Commun.* **2000**, *2*, 85−89.
(17) Holzle, M. H.; Retter, U.; Kolb, D. M. *J. Electroanal. Chem.* **1994**, *371*, 101−109.
(18) Holzle, M. H.; Zwing, V.; Kolb, D. M. *Electrochim. Acta* **1995**, *40*, 1237−1247.
(19) Radisic, A.; Vereecken, P. M.; Hannon, J. B.; Searson, P. C.; Ross, F. M. *Nano Lett.* **2006**, *6*, 238−242.
(20) Barradas, R. G.; Bosco, E. *J. Electroanal. Chem.* **1985**, *193*, 23−26.